HHS Public Access

Author manuscript

Proc SPIE Int Soc Opt Eng. Author manuscript; available in PMC 2021 February 01.

Published in final edited form as:

Proc SPIE Int Soc Opt Eng. 2020 February ; 11320: . doi:10.1117/12.2549340.

Neutrophil Extracellular Traps (NETs): An unexplored territory in renal pathobiology, a pilot computational study

Briana A. Santo[1], **Brahm H. Segal**[3], **John E. Tomaszewski**[1], **Imtiaz Mohammad**[1], **Amber M. Worral**[1], **Sanjay Jain**[4], **Michelle B. Visser**[2], **Pinaki Sarder**[1,*]

[1]Department of Pathology and Anatomical Sciences – University at Buffalo, The State University of New York

[2]Department of Oral Biology – University at Buffalo School of Dental Medicine

[3]Departments of Medicine, Immunology – Roswell Park Comprehensive Cancer Center

[4]Departments of Medicine, Nephrology – Washington University School of Medicine

Abstract

In the age of modern medicine and artificial intelligence, image analysis and machine learning have revolutionized diagnostic pathology, facilitating the development of computer aided diagnostics (CADs) which circumvent prevalent diagnostic challenges. Although CADs will expedite and improve the precision of clinical workflow, their prognostic potential, when paired with clinical outcome data, remains indeterminate. In high impact renal diseases, such as diabetic nephropathy and lupus nephritis (LN), progression often occurs rapidly and without immediate detection, due to the subtlety of structural changes in transient disease states. In such states, exploration of quantifiable image biomarkers, such as Neutrophil Extracellular Traps (NETs), may reveal alternative progression measures which correlate with clinical data. NETs have been implicated in LN as immunogenic cellular structures, whose occurrence and dysregulation results in excessive tissue damage and lesion manifestation. We propose that renal biopsy NET distribution will function as a discriminate, predictive biomarker in LN, and will supplement existing classification schemes. We have developed a computational pipeline for segmenting NET-like structures in LN biopsies. NET-like structures segmented from our biopsies warrant further study as they appear pathologically distinct, and resemble non-lytic, vital NETs. Examination of corresponding H&E regions predominantly placed NET-like structures in glomeruli, including globally and segmentally sclerosed glomeruli, and tubule lumina. Our work continues to explore NET-like structures in LN biopsies by: 1.) revising detection and analytical methods based on evolving NETs definitions, and 2.) cataloguing NET morphology in order to implement supervised classification of NET-like structures in histopathology images.

Keywords

Neutrophil Extracellular Traps; Systemic Lupus Erythematosus; Lupus Nephritis; Segmentation; Feature engineering

[*]Address all correspondence to: Pinaki Sarder, Tel: 716-829-2265; pinakisa@buffalo.edu.

1. INTRODUCTION

In the age of modern medicine and artificial intelligence (AI), image analysis and machine learning (ML) have revolutionized the field of diagnostic pathology, facilitating the development of computer aided diagnostics (CADs) such as automated classifiers for predicting disease stages. The application of ML in digital pathology circumvents existing diagnostic challenges, including image complexity and inter-observer variability. Although automated classifiers will expedite and improve the precision of clinical workflow, correlation of classifier results with outcome data in order to predict disease progression remains minimally explored. In high impact renal diseases, such as diabetic nephropathy (DN) and lupus nephritis (LN), progression often occurs rapidly and without immediate detection[1, 2], due to the subtlety of structural changes in transient disease states. In such states, exploration of quantifiable image biomarkers, such as Neutrophil Extracellular Traps (NETs)[3], may reveal highly precise and accurate progression measures which correlate with clinical data.

Systemic Lupus Erythematosus (SLE) is an autoimmune disease which predominantly affects the joints, kidneys, and other organs. Kidney inflammation due to SLE – Lupus Nephritis (LN) – remains a major risk factor for morbidity and mortality, with 10% of patients developing end-stage renal disease. LN is diagnosed, and classified, based on pathologist visual scoring of renal biopsies. Disease class (Class I–II, III A/C, IV A/C, V–VI) is assigned based on a given biopsy's frequency and distribution of active and chronic lesions[2]. LN classification and prognosis remains challenging due to lesion transformation and heterogeneity. Identification of a discriminate biomarker indicative of LN progression is paramount.

Neutrophil Extracellular Traps (NETs) have been implicated in SLE as immunogenic cellular structures, whose occurrence and dysregulation results in excessive tissue damage and lesion manifestation[4]. We propose that NET character and distribution in renal biopsies will function as a discriminate, predictive biomarker in LN, defining lesion transformation from active to chronic, and supplementing existing classification schemes. Our work aims to explore NET-like structures in LN, coincidence with LN lesions, and correlation with clinical data recorded at time of biopsy and follow-up, in order to provide a unique biomarker for progression risk scoring. To meet these aims, we have developed a computational pipeline for NET-like structures in LN biopsies.

2. METHODS

2.1 Human data.

Biopsy samples from human LN patients with disease class III, IV, and V were collected from the Kidney Translational Research Center at Washington University School of Medicine directed by Dr. Jain. Human data collection procedure followed a protocol approved by the Institutional Review Board at University at Buffalo. Biopsy samples were provided as a collection of 3–5 μm serial tissue sections mounted on glass slides. It is noted that tissue sections were formalin fixed and paraffin embedded (FFPE).

2.2 Immunofluorescence (IF) staining and imaging:

Tissue sections from LN biopsies (n = 21), Classes III, IV, and V) were labeled using: 1.) Histone H3 (H3) (Abcam, ab12079) as a primary antibody with Alexa Fluor 488 (Abcam, ab150129, ex/ em (nm): 495/519) as the secondary, and 2.) Neutrophil Elastase (NE) (Abcam, ab68672) as a primary antibody with Alexa Fluor 594 (Abcam, ab 150129, ex/ em (nm): 495/519) as the secondary. Tissue sections were spotted with DAPI mounting media (Vectashield Antifade Mounting Medium with DAPI, ex/em (nm): 358/461, Vector Laboratories, Inc) and coverslips were applied. Slides were stored for the duration at 4°C. A wide-field fluorescence microscope (DM6000B Microscope, 40X, NA = 0.85, Nuance EX Multispectral Imaging Camera, Leica Microsystems, Buffalo Grove, Il) was used to capture ROI images. Our procedure was consistent with existing protocols for IF staining in FFPE tissues[7].

2.3 Histology (H&E) post-staining and imaging:

Application of H&E post-stain to tissue sections required dissolution of mounting media and coverslip removal. This step was challenging due to the risk of damaging or disturbing the orientation of tissue mounted on the slide. Mounting media was dissolved via repeated immersion in xylene. With each immersion, the coverslip was gently and incrementally pulled back, preserving tissue integrity and orientation. Tissue sections were then stained using H&E, and imaged using a whole-slide scanner (Aperio ScanScope, 40X, Leica Microsystems, Buffalo Grove, Il) in bright-field mode.

2.4 IF Image preparation:

Per captured ROI, raw intensity images corresponding to each of the IF probes – NE, H3, and DAPI – were assigned to the red, green, and blue (RGB) channels, respectively. Channels were then merged to produce a raw RGB image. Intensity images were also thresholded to exclude extraneous signal, and merged to produce a refined RGB image. Refined RGB images were generated for downstream image analysis, whereas raw RGB images were generated for assessment of intensity image normalization.

2.5 IF Image segmentation:

Current NET detection methods define NET-positive (NET+) regions as the colocalization of IF signals for neutrophil-specific granule components (e.g. myeloperoxidase, neutrophil elastase, etc.), and nuclear components – histone, and DNA[7]. NET definitions further detail the presence of decondensed chromatin within colocalization regions[7]. In order to segment potential NETs, logical masks corresponding to specific signal in the NE, H3 and DAPI channels, were generated by thresholding each image. The intersections of these logical masks were found pairwise, and collectively: NE & H3, H3 & DAPI, NE & DAPI, NE & H3 & DAPI. The intersection of NE & H3 & DAPI provides colocalization of all NET markers, and thus preliminary NET segmentation. The H3 & DAPI mask was revised to only include objects where H3 signal exceeded DAPI, thus providing regions of decondensed chromatin. Decondensed chromatin is less compact and features exposed histone, so the intensity of DAPI signal exceeds that of H3[7]. Segmentation was refined by finding the intersection of the decondensed chromatin and preliminary NETs masks. As a result, potential NETs featuring

decondensed DNA were preserved, and all others were set to background. Size exclusion was then applied to the binary mask by setting objects with a pixel area of 100 or less to background. Structures remaining within the mask were selected for subsequent feature extraction (Figure 1). The boundary of this refined NET mask was derived, and both the mask and boundary mask were applied to the RGB IF image in order to segment and delineate NET-like structures.

2.6 Expert assessment:

Raw IF and normalized IF images, as well as images of NET-like structure segmentations, were provided to co-author Dr. Brahm Segal (an immunology and NET expert) for visual assessment.

2.7 Feature engineering:

NET-like structures were enumerated, and each structure's morphological and intensity features were extracted. Derived features included: area, eccentricity, pixel intensity statistics. Feature extraction was achieved via application of MATLAB *regionprops*.

2.8 H&E ROI extraction:

Each ROI was extracted from the corresponding H&E post-stained WSI. Boundary masks derived from segmented IF images were superimposed in order to outline NET-like structures in H&E images.

3. RESULTS

3.1 Immunofluorescence (IF) Image segmentation:

NET-like structures were segmented from refined, merged RGB images. We observed that NET-like structures were detected in regions of interest (ROIs) derived from Class III and IV ($n = 2$/class), but not Class V ($n = 2$), LN biopsies. A qualitative description of such structures includes: circular cross-sectional area, diffuse decondensed DNA, coincident neutrophil elastase and histone signal about the structure's periphery. This appearance is consistent with non-lytic NET structure, as detailed in recent SLE NET publications[3, 5, 6]. A quantitative description is provided as a part of feature extraction.

3.2 Expert assessment:

Co-author, Dr. Segal, confirmed that segmented structures were NETs. Given that our conclusions rely on expert opinion, rather than ground truth, results will be called NET-like structures.

3.3 Feature engineering:

NET-like structures were quantified in ROIs. Class III ROIs averaged 5 NET-like structures, whereas Class IV ROIs averaged 3. Features extracted from NET-like structural regions included: area, eccentricity, and pixel intensity statistics (Table 1). We attribute the subtle variation in DAPI intensity to our successful segmentation of NET-like structures featuring decondensed DNA exclusively. In addition, we hypothesize that H3 and NE distribution is

more variable due the to the random distribution of nuclear and granule components in NETs[7], both within and outside of their respective compartments, but still within the boundaries of the cell membrane. Eccentricity was computed to assess shape. Classically, NETs are defined as filamentous, or stellate[3, 7]. However, computed eccentricity suggests our NETs are more elliptical than linear. Taken together, these computed features lead us to believe that our NET-like structures are pathologically distinct. Recent literature has detailed disease specific mechanisms of NET formation resulting in morphologically distinct structures[3, 5, 6].

3.4 H&E ROI extraction:

Visualization of corresponding H&E regions (Figure 2) predominantly placed NET-like structures in glomeruli, including globally sclerosed, as well as tubule lumina. Sclerosis was confirmed via examination of adjacent Periodic acid-Schiff (PAS) stained sections. Few NET-like structures presented in higher vasculature.

4. DISCUSSION

NET occurrence in LN remains minimally explored due to challenges posed by staining, imaging, and renal tissue complexity. In this work, we employed several strategies in order to navigate such challenges. NET detection methods stipulate colocalization of multiple nuclear and cytoplasmic components[7], therefore primary and secondary antibodies must be carefully selected in order to ensure distinct host species. In addition, LN biopsies readily available for research applications are frequently FFPE samples, imposing yet another restriction on antibody selection. In order to achieve successful, specific staining of our LN samples, antibody optimization employed tissue identical to experimental, antigen retrieval was completed, and experimental controls included disease and antibody level specificity. Imaging challenges, such as the risk of FRET and channel bleed-through, were minimized via careful selection of fluorescent probes and filter cubes, with distinct excitation and emission spectra.

IF analysis of diseased renal tissue is incredibly complex, and laden with extraneous positive signal, due to differential expression of similar markers and aggregated debris. Concomitantly, NETs are heterogeneous, amorphous structures, indistinguishable from surrounding tissue in traditional stains. To reduce the likelihood of false positive segmentation, our NETs analysis: 1) operated on an ROI basis, as IF whole slide imaging is noisy, 2) excluded ROIs at or near the tissue boundary, 3) eliminated extraneous signal due to uneven illumination or auto fluorescence, 4) excluded structures lacking colocalization and decondensed DNA, and 5) excluded structures with areas outside of biological feasibility. Our study integrating in-depth staining, imaging, and image analysis also mapped segmented NET-like structures from IF ROIs, to corresponding H&E post-stained regions, thus providing a focal point for further structural analysis in histopathology images and improving our understanding of NET functional contribution to disease progression.

5. CONCLUSION AND FUTURE WORKS

Our work not only provides for automated, computational assessment of NETs in *ex vivo* samples, but also successfully quantifies NET-like structures in LN biopsies. To our knowledge, this is one of the earliest works enabling examination of NET-like structures in traditionally (H&E) stained LN biopsies. As a direct result, NET quantification via our analysis will enable implementation of supervised classification for classifying NET-like structures in LN histopathology images. Also, confirmation of NETs as biomarkers in LN progression potentiates NETs as candidates for targeted therapy. We recognize that the applied staining method, although considered to be gold standard, is tailored to the classical definition of NETs and NETosis[3, 5, 7]. We also recognize that recent developments in neutrophil biology have identified non-lytic, vital NET formation as a unique immuno-pathologic process in SLE[3, 5, 6]. Vital NET formation preserves the integrity of the cell's plasma membrane by exporting nuclear and granule components via cytoplasmic blebbing, and thus manifests as a spherical structure with colocalization of distinct biomarkers. Our segmented NET-like structures fit this profile. This observation warrants further study, and will be the focus of future work.

ACKNOWLEDGEMENTS

The project was supported by the faculty startup funds from the Jacobs School of Medicine and Biomedical Sciences, University at Buffalo; Buffalo Blue Sky grant, University at Buffalo; NIDDK Diabetic Complications Consortium grant U24 DK076169; NIDDK grant R01 DK114485 & DK114485 02S1; and NIDDK CKD Biomarker Consortium grant U01 DK103225. We acknowledge the assistance of the Multispectral Imaging Suite and Histology Core Laboratory in the Dept. of Pathology & Anatomical Sciences, Jacobs School of Medicine and Biomedical Sciences, University at Buffalo.

REFERENCES

[1]. Tervaert TWC, Mooyaart AL, Amann K et al., "Pathologic classification of diabetic nephropathy," CJASN, 21(4), 556–563 (2010).

[2]. Weening JJ, D'Agati VD, Schwartz MM et al., "The classification of glomerulonephritis in systemic lupus erythematosus revisited," CJASN, 15(2), 241–250 (2004).

[3]. Boeltz S, Amini P, Anders H-J et al., "To NET or not to NET: current opinions and state of the science regarding the formation of neutrophil extracellular traps," Cell Death & Differentiation, 26(3), 395–408 (2019). [PubMed: 30622307]

[4]. Almaani S, Meara A, and Rovin BH, "Update on lupus nephritis," CJASN, 12(5), 825–835 (2017). [PubMed: 27821390]

[5]. Konig MF, and Andrade F, "A critical reappraisal of neutrophil extracellular traps and NETosis mimics based on differential requirements for protein citrullination," Frontiers in Immunology, 7, 461(2016). [PubMed: 27867381]

[6]. van Dam LS, Kraaij T, Kamerling SWA et al., "Neutrophil extracellular trap formation is intrinsically distinct in ANCA - associated vasculitis and systemic lupus erythematosus," Arthritis & Rheumatology, (2019).

[7]. Brinkmann V, Abu Abed U, Goosmann C et al., "Immunodetection of NETs in paraffin-embedded tissue," Frontiers in Immunology, 7, 513(2016). [PubMed: 27920776]

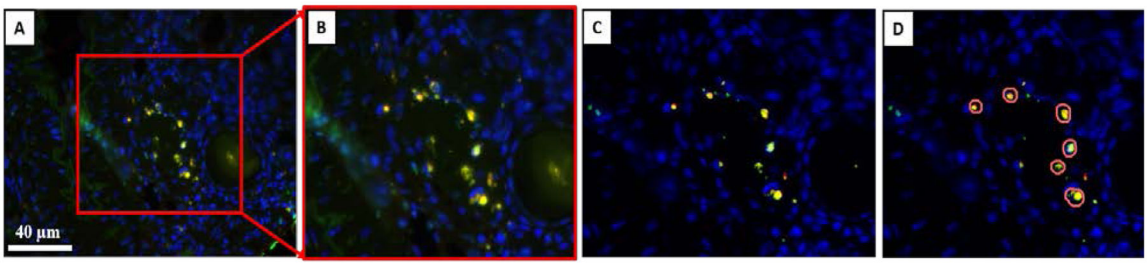

Figure 1: Automated Segmentation of NET-Like Structures in Lupus Nephritis Biopsies, based on Biopsy Regions of Interest

A) RGB Image: Initial Merged IF with NE, H3, and DAPI assigned to the red(R), green(G), and blue(B) channels, respectively. B) RGB Image: Cleaned-Up Merged IF. C) Colocalization of NE, H3, and DAPI, where intensity of H3 > DAPI. D) RGB Image and Boundary: Segmented NET-Like Structures.

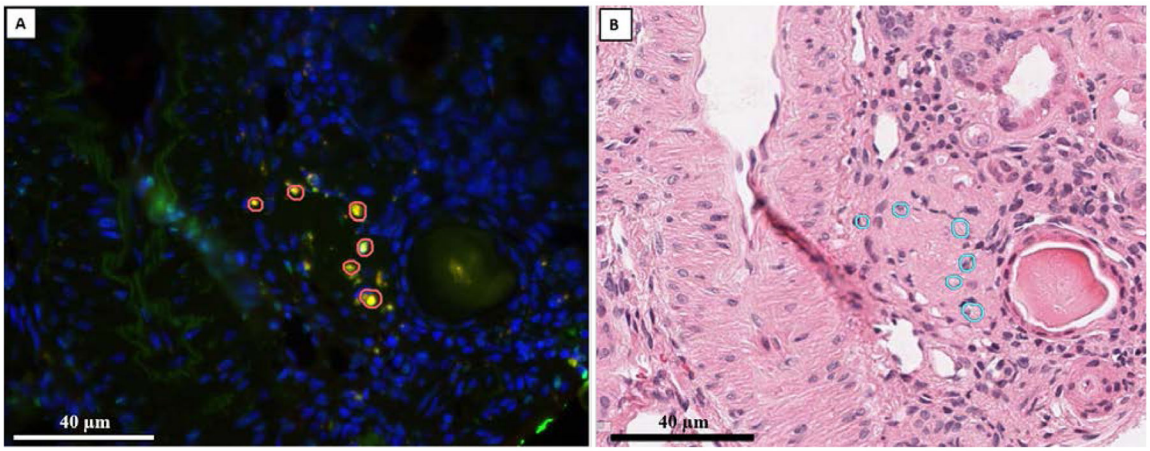

Figure 2: NET-Like structure boundary segmentation in immunofluorescence and histology images.

A) IF Image B) Bright field Image, H&E. NET-like structure boundaries are shown in red and blue.

Table 1:

NET-like Structure Features.

Neutrophil Elastase (NE), Histone H3 (H3), DNA (DAPI). Intensity refers to pixel intensity. All values calculated as an average across ROIs. Variation calculated as difference in maximum and minimum intensity values per ROI, then averaged across ROIs. Error bar indicates standard deviation across ROIs.

NET-Like Structure Features	Class III ROIs	Class IV ROIs	Collective ROIs
Quantity	5.25±2.4	3.68±3	3.96±2.9
Area (μm^2)	20.90±5.6	16.01±11	16.87±11
Eccentricity	0.72±.08	0.58±0.29	0.61±0.27
Variation NE Intensity	109.34±15	79.56±43	84.86±41
Variation H3 Intensity	102.40±18	86.41±44	89.25±41
Variation DAPI Intensity	51.29±30	39.62±26	41.69±27